Power System Restoration Planning with Standing Phase Angle and Voltage Difference Constraints

Terrence W.K. Mak*, Carleton Coffrin†, Pascal Van Hentenryck‡, Ian A. Hiskens§, and David Hill¶
* NICTA & University of Melbourne, Australia. (Terrence.Mak@nicta.com.au)
† NICTA, Australia. (carleton.coffrin@nicta.com.au)
‡ NICTA & The Australian National University (pvh@nicta.com.au)
§ University of Michigan, Ann Arbor, MI 48109, USA. (hiskens@umich.edu)
¶ University of Hong Kong, Central, Hong Kong. (dhill@eee.hku.hk)

***Abstract*— This paper considers the restoration of a transmission system after a significant disruption such as a natural disaster. It considers the Restoration Order Problem (ROP) that jointly considers generator dispatch, load pickups, and restoration prioritization to minimize the size of the blackout while satisfying the network operational constraints. The paper examines transient effects in power restoration and generalizes the ROP formulation with standing phase angle and voltage difference constraints in order to minimize rotor swings. Case studies indicated that the novel ROP-SPASVD formulation reduces rotor swings of synchronous generators by over 50%, while having a negligible impact on the blackout size (i.e., $\leq$ 1.5% increase), which is still optimized holistically.**

***Keywords*—Power System Restoration, Standing Phase Angle, Generator Dynamics, DC Power Flow, LPAC Power Flow, Mixed-Integer Nonlinear Programming**

NOMENCLATURE

$V = v + i\theta$	AC voltage
$S = p + iq$	AC power
$Z = r + ix$	Line resistance
$Y = g + ib$	Line admittance
$V = \|V\|\angle\theta^\circ$	Polar form
$\mathcal{PN}$	Power network
N	Set of buses in a power network
$N(n)$	Set of buses connected to bus n by a line
D	Set of demand points in a power network
$D(n)$	Set of demands at bus n
G	Set of voltage controlled generators
$G(n)$	Set of generators at bus n
L	Set of lines $\langle n, m\rangle$ in a power network where n is the form node
L^r	Set of lines $\langle n, m\rangle$ in a power network where n is the to node
A	All network components ($N \cup L \cup D \cup G$)
$\mathcal{D}$	Damaged components in the network
$\mathcal{R} \subseteq \mathcal{D}$	Network components selected for repair
s	Slack bus
θ°_{ij}	Shorthand for $\theta^\circ_i - \theta^\circ_j$
V_{ij}	Shorthand for $\|V_i\| - \|V_j\|$
θ^Δ	Maximum Standing Phase Angle
V^Δ	Maximum Standing Voltage Diffrence
μ	Average
$\overline{x}$	Upper bound of x
$\underline{x}$	Lower bound of x

I. INTRODUCTION

Restoring a transmission system after a significant disruption, e.g., a cascading voltage collapse or a natural disaster, is an important task with consequences on both human and economic welfare. However, restoration plans are very challenging to design: Planners aim at minimizing the blackout period but also must prioritize repairs (i.e., determine the order in which to energize lines), load pickups, and generator dispatch without violating static network constraints (e.g., line thermal limits) and creating significant transient effects (e.g., large rotor swings).

This paper is part of a long-term research project [1]–[4] to develop holistic power restoration algorithms for responding to significant network disruptions, such as those stemming from natural disasters. Past research has isolated a key sub-problem in power system restoration, the Restoration Ordering Problem (ROP) [3], which formalizes the process of prioritizing network repairs, re-dispatching generations, and picking up new loads to minimize the blackout period. The ROP determines the best sequence of steady states, each state associated with a restoration action. It raises significant computational challenges: Since no *typical* operating point is known for the damaged network, even determining a sequence of steady states that satisfy the AC power flow equations is a non-trivial endeavor and the popular DC power flow approximation cannot be used in this context [4]. To remedy this limitation, prior and existing work introduced and use the LPAC model to obtain a more accurate approximation to the AC power flow equations [4], [5].

Prior work on the ROP problem restricts attention to determining an optimal sequence of AC-feasible steady-states: It did not consider whether the power system can transition from each steady-state to the next. This is important issue however since, in a restoration context, the power network is operating far from its original design specification and many topology changes are occurring. This paper is a first step in addressing transient effects during the computation of high-quality restoration plans for the ROP problem. Inspired by field practices [6]–[10], it proposes an enhanced formulation of the ROP to mitigate dynamic rotor swings (one of many possible transient effects to consider) by imposing standing phase angle (SPA) and voltage difference (SVD) constraints. The formulation splits each restoration action into two steps as illustrated in Figure 1: *A dispatch step* where the generation dispatch and load pickups are adjusted to meet the SPA

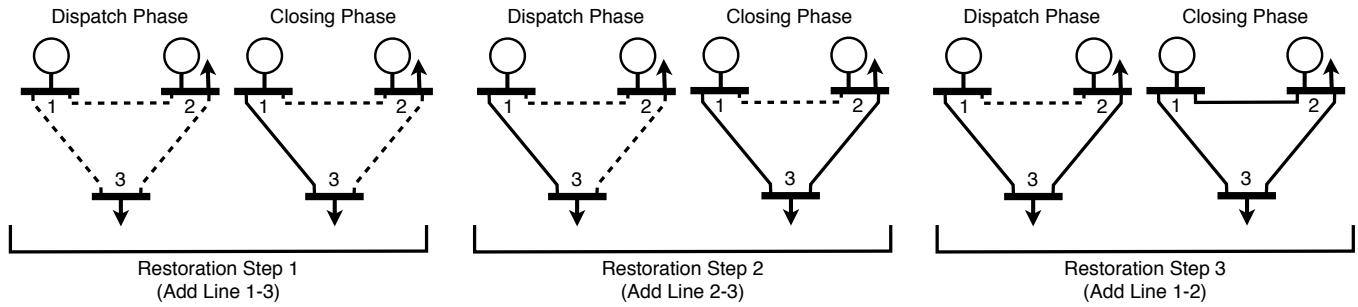

Fig. 1. The Two Phases of the Restoration Ordering Algorithm.

and SVD constraints and *a closing step* where the repaired component is energized. The resulting formulation is called the ROP-SPASVD formulation. The benefits of the ROP-SPASVD formulation are evaluated using the commercial transient simulator POWER WORLD [11], [12] and five MATPOWER test systems [13]. The key findings can be summarized as follows: (1) The DC power flow approximation is not appropriate for solving the ROP-SPASVD, while the LPAC model has the required accuracy. (2) SPA and SVD constraints can reduce rotor swings of synchronous generators by over 50%. (3) By jointly considering SPA and SVD constraints with load pickups and generation dispaches, improvements in rotor swings have negligible impacts on the blackout size (i.e., $\leq 1.5\%$ increase), which is optimized holistically.

II. PRIOR WORK

SPA constraints have been proposed before to improve rotor stability. Most of the work on SPA constraints [8]–[10] focuses on methods and algorithms to minimize the standing phase angle for restoring one selected transmission line only. Ye and Liu [10] allow unserved load to be picked up during the restoration as a control strategy to minimize the SPA, which is natural in power restoration [3]. They also use the AC non-linear power flow equations. In contrast, this research considers the restoration prioritization globally and imposes SPA constraints for the damaged lines over the course of the restoration. The rotor swings are analyzed globally over the entire restoration process. This research also uses the LPAC model [5] to approximate the power flow equations, which allows the entire restoration process to be expressed as a mixed-integer program, which is more tractable than a mixed integer non-linear program. This research also shows that SPA constraints may not be sufficient in reducing rotor swings and considers SVD constraints to remedy this limitation.

III. MODELING ROTOR SWINGS

This paper adopts the "classical" model of generator dynamics combined with the following swing equation [14]:

$$\frac{2H}{\omega_0}\frac{d^2\delta}{dt^2} = P^m - P^e - D\omega$$

where H, δ, D, ω, and ω_0 is the inertia constant, rotor angle (in terms of electrical angle), the damping coefficient, the current angular velocity, and the nominal angular velocity of the synchronous machine. On the right hand side, P^m and P^e are the mechanical and electrical power acting on the rotor

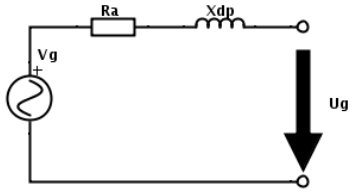

Fig. 2. Circuit diagram of classical generator model

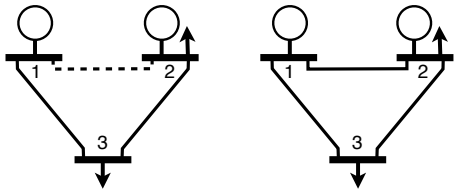

Fig. 3. Topology Change Example: Open State (left), Closed State (right).

of the generator. The circuit of the "classical" model of a generator is shown in Figure 2. U_g and V_g are the constant voltage supplied by the generator and the voltage of the bus the generator is being connected to. R_a and X_{dp} are the armature resistance and the transient reactance of the generator. By using U_g, V_g, R_a, and X_{dp} following the circuit diagram, we could compute P^e. The paper also uses the PTI IEEE dynamic load model [15] when performing simulations. The load model changes the active and reactive power of the load depending on the voltage and frequencies shown in the following equation:

$$p^{l'} = p^l[a_1(\frac{V_l}{V_0})^{n_1} + a_2(\frac{V_l}{V_0})^{n_2} + a_3(\frac{V_l}{V_0})^{n_3}][1 + a_7\Delta f]$$
$$q^{l'} = q^l[a_4(\frac{V_l}{V_0})^{n_4} + a_5(\frac{V_l}{V_0})^{n_5} + a_6(\frac{V_l}{V_0})^{n_6}][1 + a_8\Delta f]$$

where p^l and q^l is the amount of active and reactive power served at steady state and $p^{l'}$ and $q^{l'}$ is the resulting active and reactive power demand. V_l and V_0 are the voltage of the bus the load is currently connected to and the nominal voltage of the system. Δf is the change in frequency of the power network. All variables a_i ($i \in \{1..8\}$) and n_j ($j \in \{1..6\}$) are configurable constants.

IV. TOPOLOGY CHANGES AND ROTOR SWINGS

To build the intuition behind the ROP-SPASVD model, consider the 3-bus network in Figure 3 and its parameters in Tables I. This 3-bus example is in fact a sub-graph of the IEEE

TABLE I. LINE, LOAD, AND GENERATOR MODEL PARAMETERS

Line	R	X	B
1 to 2	0.01938	0.05917	0.00000
1 to 3	0.05403	0.22304	0.00000
2 to 3	0.05695	0.17388	0.00000

Load	MW	Mvar
Bus 2	100.00	0.00
Bus 3	100.00	0.00

Generator	H	D	Ra	Xdp
Gen 1	30.00	5.00	0.02	0.20
Gen 2	30.00	5.00	0.02	0.20

TABLE II. RESTORATION CASE: SETTINGS

Case	Bus 1	Bus 2	Bus 1	Bus 2	Gen 1 Pow.	Gen 2 Pow.	1st Swing
	Volt.(kV)	Volt.(kV)	Ang.(deg)	Ang.(deg)	(MW/Mvar)	(MW/Mvar)	(deg)
1	146.28	97.24	0.00	-47.58	221.12/143.46	20.00/18.00	44.229
2	146.28	146.28	0.00	-35.33	207.42/28.05	20.00/78.32	31.249
3	146.28	141.725	0.00	-12.14	102.59/10.66	102.59/10.66	10.385
4	146.28	123.84	0.00	0.00	61.05/48.08	143.85/-30.00	0.619
5	146.28	146.28	0.00	0.00	45.37/6.10	157.31/3.16	0.002

14 standard test case. This section conduct two studies on this network: (1) a restoration topology change (i.e., adding line 1–2); and (2) a congestion removing topology change (i.e., removing line 1–2). The effects of the topology change is evaluated on five scenarios, each of which correspond to a different generator dispatch that meets the load. Scenario 5 is a dispatch that produces the same phase angles and voltage magnitudes for the generator buses. Scenario 2 (resp. 4) is a dispatch where the magnitudes (resp. the angles) are the same for the generator buses. Scenario 3 has the same dispatch for both generator. Scenario 5 is a dispatch with no specific constraint. In this study, a swing of more than 90 degrees is unacceptable and should lead to self-protection measures [14].

In restoration, the network starts in the open state (Figure 3 - left) and, after 10 seconds, the line breaker is closed (Figure 3 - right). Table II reports the first rotor swing of generator 1 for each of the five scenario. The results show that, as standing phase angle differences increase, so do the generator swings. Figure 4 depicts the rotor angles of generator 1 for the scenarios. The figure clearly shows that the swing increases drastically with large phase angle differences. Hence, it is obviously desirable to select generator dispatch with small angle differences in power restoration. In line switching, the network starts in the closed state (Figure 3 - right) and, after 10 seconds, the line breaker is opened. Table III and Figure 5 present the results. The results are similar to the restoration case but more extreme. In particular, the first two scenarios lead to instabilities in the network, while smaller SPAs and SVDs reduce the rotor swing and achieve stability.

V. POWER RESTORATION ORDERING PROBLEM WITH STANDING PHASE ANGLE CONSTRAINTS

Section IV confirmed standard field practices [6]–[10]. and suggests to enhance the ROP formulation in [3] with SPA and SVD constraints in order to mitigate rotor swings. The ROP-SPASVD includes two extensions. First, the model must be extended to the AC power flow equations for the reasons stated in [4] and discussed below. Second, to incorporate the effects of SPA constraints, each restoration step must be broken into two phases: A *dispatch* phase d and a *closing* phase c. The goal of the dispatch phase is to re-dispatch the generators to

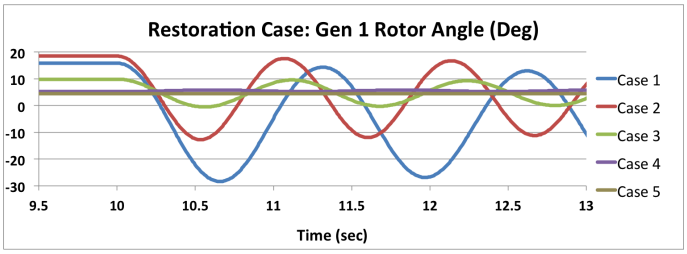

Fig. 4. Restoration Case: Generator 1 Rotor Angle

TABLE III. REMOVAL CASE: SETTINGS

Case	Bus 1	Bus 2	Bus 1	Bus 2	Gen 1 Power	Gen 2 Power	1st Swing
	Volt.(kV)	Volt.(kV)	Ang.(deg)	Ang.(deg)	(MW/Mvar)	(MW/Mvar)	(deg)
1	146.28	142.36	0.00	-4.23	206.27/20.88	0.00/0.63	>90(unstable)
2	146.28	146.28	0.00	-4.62	206.48/-36.62	0.00/58.70	>90(unstable)
3	146.28	145.22	0.00	-1.50	101.53/5.40	101.53/5.40	10.276
4	146.28	143.01	0.00	0.00	60.06/50.59	143.00/-40.00	0.137
5	146.28	146.28	0.00	0.00	45.28/6.13	157.40/3.13	0.016

satisfy the SPA and SVD constraints for the repaired line. The closing phase adds the repaired line to the network and ensures that all operational constraints are satisfied. The closing phase enforces the generator dispatch selected in the dispatch phase.

A complete model for the AC-ROP-SPASVD is presented in Model 1. The model assumes the components of the network will be energized one at a time and will remain energized for the remainder of the restoration process. The restoration is modeled as $2|\mathcal{R}|$ steady states, with one dispatch phase and one closing phase for each of the $|\mathcal{R}|$ restoration actions. Note that each measure (e.g., real power on a line (i, j)) is associated with $2|\mathcal{R}|$ variables, one for each restoration step r and phase p. As the input data and variables of the AC-ROP-SPA are described in Model 1 in detail, only the constraints are discussed. The objective (O.1) strives to reducing the size of the blackout and thus to serve as much active power as possible through the restoration process. Constraints (C.1.x) are concerned with the operational state of the components in the network. Constraints (C.1.1) ensure all non-damaged components are active, while Constraints (C.1.2) ensure components not selected for repair remain inactive. Constraints (C.1.3) activate one component in each time step, and Constraints (C.1.4) ensure components remain active in future time steps. Constraints (C.1.5)–(C.1.7) capture the operational state of the components. A component is only operational after it and all of its dependent parts are active. Constraints (C.2.x) model the AC power flow equations and link them with the operational state of the network. Constraints (C.2.1) selects a slack bus. Constraints (C.2.2)–(C.2.3) model Kirchhoff's Current Law and Constraints (C.2.4)–(C.2.5) capture the flow of power by Ohm's Law. Constraints (C.2.6) capture the line thermal limits. Constraints (C.2.7)–(C.2.9) link the operational state of the generators and loads to the power flow variables. Finally, Constraints (C.3.x) model the constraints between simulation phases. Constraints (C.3.1)–(C.3.2) fix the generator dispatch between the phases. Constrains (C.SPA) implements a standing phase angle constraint of less then θ^{Δ} when a line is closed in step r. While constraints (C.SVD) implements a similar voltage difference constraint. The AC-ROP-SPASVD jointly considers generator dispatch, load pickups, topology changes,

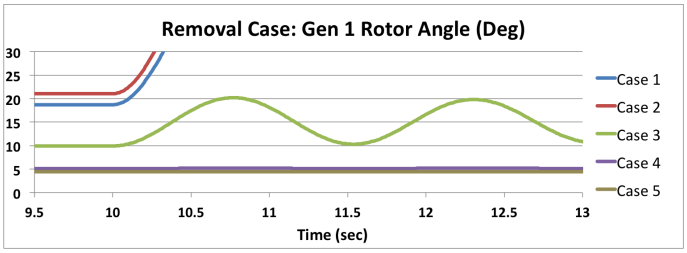

Fig. 5. Removal Case: Generator 1 Rotor Angle

TABLE IV. BLACKOUT SIZE AND CONVERGENCE RATE FOR THE DC-ROP-SPA.

	6 Bus (Complete Search)		14 Bus (2 hr Limited Search)	
θ^{Δ} Deg	Blackout (%)	# Failed / Total	Blackout (%)	# Failed / Total
180	12.55	3 / 6	5.35	2 / 7
10	12.55	1 / 6	5.35	2 / 7
5	12.55	2 / 6	5.35	1 / 7
2.5	12.55	2 / 6	5.35	1 / 7
1.25	12.55	1 / 6	5.35	2 / 7

restoration prioritization and the network operation limits. It also uses SPA and SVD constraints to improve transient stability in generator dynamics model.

The AC-ROP-SPA is a challenging Mixed-Integer non-convex Non-linear Program (MINLP) which is outside the scope of modern global optimization tools. To address its computational challenges of solving the AC-ROP-SPA globally, a natural avenue is to approximate the power flow equations. For instance, the AC-ROP was approximated with the popular DC power flow model in [3], resulting in a mixed-integer program (MIP) formulation which exploits mature industrial tools. Unfortunately, a DC-ROP-SPA approximation of the AC-ROP-SPA produces restoration plans riddled with problems: The DC solutions to the power flow equations could not be converted in AC solutions and the SPA constraints did not reduce rotor swings. (SVD constraints cannot be expressed in the DC model.) These observations, which are consistent with prior work in power restoration [4], [9], [10], are illustrated in Table IV. The table gives the SPA limit, the size of the blackout in percentage, and the number of times a DC plan cannot be converted into an AC plan for the 6 bus and the 14 bus case studies. Observe that the backout area does not change as the SPA constraints become tighter, highlighting again that the DC model is not accurate enough to reason on the bus phase angles in a restoration context.

To remedy these issues, this paper uses the LPAC model [5] to model the power flow equation as suggested in [4]. The LPAC model approximates the AC power flow with a linear program, captures reactive and volatge magnitudes, and is derived from the following assumptions: (1) $\sin(\theta^{\circ}_n - \theta^{\circ}_m) \approx \theta^{\circ}_n - \theta^{\circ}_m$; (2) the voltage magnitude at each bus is expressed as a deviation from a nominal operating voltage, i.e., $|\widetilde{V}| = |\widetilde{V}^t| + \phi$; (3) the non-convex cosine function is replaced with a polyhedral relaxation denoted by $\widehat{\cos}_{nm}$; (4) the remaining non-linear terms are factored and approximated with a first-order Taylor expansion. The cold-start LPAC model yield the following power flow equations:

$$p_{nm} = g_{nm} - g_{nm}\widehat{\cos}_{nm} - b_{nm}(\theta^{\circ}_n - \theta^{\circ}_m)$$
$$q_{nm} = -b_{nm} + b_{nm}\widehat{\cos}_{nm} - g_{nm}(\theta^{\circ}_n - \theta^{\circ}_m) - b_{nm}(\phi_n - \phi_m)$$

Model 1 The ROP with SPA and SVD Constraints

Inputs:

$\mathcal{PN} = \langle N, L, G, D, s\rangle$ -Power network
$\mathcal{D}, \mathcal{R}$ -Damaged & restored items
Variables: $(0 \le r \le |\mathcal{R}|, p \in \{d, c\})$
$y_{ri} \in \{0,1\}, \forall i \in A$ - Item i is repaired at step r
$z_{ri} \in \{0,1\}, \forall i \in A$ - Item i is operational at step r
$\theta_{rpi} \in (-\infty, \infty), \forall i \in N$ - Bus i angle at step r phase p
$V_{rpi} \in (\underline{V}_i, \overline{V}_i), \forall i \in N$ - Bus i voltage at step r phase p
$l_{rpi} \in (0,1), \forall i \in D$ - Load i precent at step r phase p
$p^g_{rpi} \in (0, \overline{p}^g_i), \forall i \in G$ - Active injection of generator i
$q^g_{rpi} \in (\underline{q}^g_i, \overline{q}^g_i)$, $\forall i \in G$ - Reactive injection of generator i
$p_{rpij} \in (-\overline{S}_k, \overline{S}_k), \forall \langle k : i, j\rangle \in L \cup L^r$ - Active flow on line k
$q_{rpij} \in (-\overline{S}_k, \overline{S}_k), \forall \langle k : i, j\rangle \in L \cup L^r$ - Reactive flow on line k

Maximize

$$\sum_{r=0}^{|\mathcal{R}|} \sum_{p\in\{d,c\}} \sum_{i\in D} \overline{p}^l_i l_{rpi} \tag{O.1}$$

Subject to: $(0 \le r \le |\mathcal{R}|, p \in \{d, c\})$

$$y_{ri} = 1, \quad \forall i \in A\backslash\mathcal{D} \tag{C.1.1}$$
$$y_{ri} = 0, \quad \forall i \in \mathcal{D}\backslash\mathcal{R} \tag{C.1.2}$$
$$\sum_{i\in\mathcal{D}} y_{ir} = r, \tag{C.1.3}$$
$$y_{(r-1)i} \le y_{ri}, \quad \forall i \in \mathcal{D}, r \ne 0 \tag{C.1.4}$$
$$z_{ri} = y_{ri}, \quad \forall i \in N \tag{C.1.5}$$
$$z_{ri} = y_{ri} \wedge y_{rj}, \quad \forall j \in N, \forall i \in G(j) \cup D(j) \tag{C.1.6}$$
$$z_{rk} = y_{rk} \wedge y_{ri} \wedge y_{rj}, \quad \forall \langle k : i, j\rangle \in L \tag{C.1.7}$$
$$\theta_{rps} = 0 \tag{C.2.1}$$
$\forall i \in N$
$$\sum_{j\in G(i)} p^g_{rpi} - \sum_{j\in L(i)} \overline{p}^l_i l_{rpi} = \sum_{j\in N(i)} p_{rpij} \tag{C.2.2}$$
$$\sum_{j\in G(i)} q^g_{rpi} - \sum_{j\in L(i)} \overline{q}^l_i l_{rpi} = \sum_{j\in N(i)} q_{rpij} \tag{C.2.3}$$
$\forall \langle k : i, j\rangle \in L \cup L^r$,
$$p_{rpij} = z_{rk}(g_{ij}V^2_{rpi} - V_{rpi}V_{rpj}(g_{ij}\cos(\theta_{rpij}) - b_{ij}\sin(\theta_{rpij}))) \tag{C.2.4}$$
$$q_{rpij} = z_{rk}(-b_{ij}V^2_{rpi} - V_{rpi}V_{rpj}(g_{ij}\sin(\theta_{rpij}) - b_{ij}\cos(\theta_{rpij}))) \tag{C.2.5}$$
$$p^2_{rpij} + q^2_{rpij} \le \overline{S}_k z_{rk} \tag{C.2.6}$$
$$\neg z_{ri} \to p^g_{rpi} = 0, \quad \forall i \in G \tag{C.2.7}$$
$$\neg z_{ri} \to q^g_{rpi} = 0, \quad \forall i \in G \tag{C.2.8}$$
$$\neg z_{ri} \to l_{rpi} = 0, \quad \forall i \in D \tag{C.2.9}$$
$$p_{rdi} = p_{(r-1)ci}, \quad \forall i \in G, r \ne 0 \tag{C.3.1}$$
$$q_{rdi} = q_{(r-1)ci}, \quad \forall i \in G, r \ne 0 \tag{C.3.2}$$
$$z_{rk} \wedge \neg z_{(r-1)k} \to |\theta_{rdij}| \le \theta^{\Delta}, \quad \forall \langle k : i, j\rangle \in L, r \ne 0 \tag{C.SPA}$$
$$z_{rk} \wedge \neg z_{(r-1)k} \to |V_{rdij}| \le V^{\Delta}, \quad \forall \langle k : i, j\rangle \in L, r \ne 0 \tag{C.SVD}$$

This work uses the warm-start LPAC model, a slightly more advanced formulation that exploits the target voltage magnitudes for more accuracy [5]. The resulting LPAC-ROP-SPA formulation is also a MIP model which remedies the limitations of the DC power flow and is sufficiently accurate to study the AC-ROP-SPA. The LPAC-ROP-SPA formulation is still very challenging computationally even for small networks (e.g., with more than 40 lines), since it holistically sequences the repairs. A randomized adaptive decomposition (RAD) [16], [17] procedure was proposed in [18] for solving

similarly challenging ROP problems. The algorithm begins with an arbitrary restoration prioritization as a starting point. It then inspects contiguous subsections of the restoration steps randomly and replaces them with improved subsections. This process is repeated several times until a fix-point is reached. This procedure lead to high quality restoration plans outside the scope of existing MIP technology [18] and is used in this paper for scaling the LPAC-ROP-SPA to larger networks.

VI. Case Studies

This section evaluates restoration plans produce by the ROP-SPA algorithm using the commercial transient simulation software POWER WORLD. It considers five well-studied power networks: the 6-bus, 9-bus, 14-bus, 30-bus, and the 50-bus[1] networks from MATPOWER [13]. For simplicity, it is assumed that the entire network has been destroyed and must be reconstructed from scratch. The restoration plans are quite detailed: They include an ordered list of repairs each with generation dispatch and load pickups. Many aspects of these plans need not be concerned with respect to transient dynamics. Hence this section makes the following assumptions: (1) standard procedures are used for connecting generators to the network; (2) large load pickups are brought up incrementally within the spinning reserve of existing generating units; (3) there is sufficient time to make significant re-dispatch of the generation units between topology changes; (4) Connecting two isolated islands is accomplished with standard procedures for matching the bus phases, voltages, and frequencies. Given these assumptions, the key restoration step with respect to the dynamic simulation is the closing of a line within a connected network, which is precisely the case described in Section IV. Hence our dynamic simulation study focuses only on these restoration steps in the ROP plans.

Given these assumptions, the experimental evaluation proceeds as follows. The ROP algorithm produces a restoration plan of $|\mathcal{R}|$ steps (as discussed in Section V). These restoration steps are filtered to the subset $\mathcal{R}'$ of line closings within connected networks. Each restoration step $r \in \mathcal{R}'$ defines a dispatch and a closed steady-state power flow on a subnetwork. The dispatch state is encoded into the POWER WORLD transient simulator with an appropriate line closing event after 10 seconds. The system dynamics are simulated for 50 seconds and the rotor swings δ_t are observed for each time t in the 10–40 second time range. To summarize the rich simulation data, only the largest rotor swing $\max_t \delta_t$ of a generator is reported. Furthermore, the results may only report the maximum or average swing values over all generators, i.e., $\max_{i\in G} \max_t \delta_{it}$, and $\mu_{i\in G} \max_t \delta_{it}$. To be consistent with field practices, this section first focuses on the effects of SPA constraints and then considers SVD constraints.

A. Swing Reduction on Fixed Restoration Order

This section first considers the case where the order of component restoration is fixed. This simplifies the computational complexity significantly since the resulting optimization is a linear program. However, the resulting restoration algorithm still produces non-trivial restoration plans since it must choose generation dispatch and load pick-ups that satisfy the SPA constraints. The key findings are: (1) even with a fixed restoration order, SPA constraints can significantly reduce rotor swings; (2) The rotor swing benefits come with a relatively small increase to the size of the blackout period. Table V summarizes the results for increasingly stronger SPA constraints (i.e., $\theta^\Delta = 180, 10, 5, 2.5, 1.25, 0.625$, and 0.3125 deg.). The case with $\theta^\Delta = 180$ is a baseline with no binding phase angle constraints. The table reports three key metrics: (1) the runtime of the linear program; (2) the blackout period percentage defined as

$$1 - \frac{\sum_{r=1}^{|\mathcal{R}|} \sum_{p\in\{d,c\}} \sum_{i\in D} \overline{p}_i^l l_{rpi}}{2|\mathcal{R}| \sum_{i\in D} \overline{p}_i^l}$$

and (3) the relative blackout change, i.e., the changes in blackout percentage compared to initial value in the baseline. The runtimes are consistent for all SPA constraints. In absolute terms, the SPA constraints produce very small increases in the size of the blackout (less than 1.5%) in all cases. Even in relative terms (Δ), the increases tend to be less than 2%, except for the 14-bus case. Figure 6 shows the maximum rotor swing of each generator for the restoration plans of outlined in Table V. The various generators in each scenario may have significantly different swing sizes. However, as the SPA constraints become tighter, the swing sizes for all generators decrease consistently by at least 50%.

TABLE V. RUNTIME & BLACKOUT ON A FIXED RESTORATION ORDER FOR DECREASING SPA VALUES

	6 Bus			9 Bus		
θ^Δ Deg	Runtime (sec)	Blackout (%)	Δ (%)	Runtime (sec)	Blackout (%)	Δ (%)
180	0.6544	32.9574	0.0000	0.4220	75.4754	0.0000
10	0.3961	32.9574	0.0000	0.3515	75.4754	0.0000
5	0.3961	32.9574	0.0000	0.3613	75.4754	0.0000
2.5	0.4045	32.9984	0.1244	0.3402	75.4754	0.0000
1.25	0.3947	33.2189	0.7935	0.3458	75.6439	0.2232
0.625	0.3940	33.3974	1.3351	0.3432	75.8203	0.4569
0.3125	0.3931	33.5618	1.8338	0.3464	75.9084	0.5738
	14 Bus			30 Bus		
θ^Δ Deg	Runtime (sec)	Blackout (%)	Δ (%)	Runtime (sec)	Blackout (%)	Δ (%)
180	1.3987	7.0319	0.0000	7.7102	21.6491	0.0000
10	1.4079	7.0319	0.0000	7.8439	21.6491	0.0000
5	1.4232	7.3180	4.0683	7.1286	21.6542	0.0234
2.5	1.5238	7.8373	11.4537	6.9371	21.7393	0.4165
1.25	1.3794	8.1258	15.5559	6.9037	21.8318	0.8438
0.625	1.7926	8.2787	17.7307	7.8398	21.8817	1.0745
0.3125	1.6328	8.3573	18.8483	8.8293	21.9124	1.2162
	50 Bus					
θ^Δ Deg	Runtime (sec)	Blackout (%)	Δ (%)			
180	29.4282	15.2453	0.0000			
10	29.6926	15.2454	0.0000			
5	29.9359	15.2556	0.0675			
2.5	29.3471	15.2679	0.1481			
1.25	30.2583	15.2765	0.2041			
0.625	29.9991	15.2828	0.2457			
0.3125	29.6855	15.2866	0.2704			

B. Swing Reduction on Flexible Restoration Order

This section considers the full ROP program that jointly optimize the prioritization of restoration, generator dispatch, and load pickups. It starts with the small networks that can be solved optimally and then move to the larger networks that are solved using randomized adaptive decomposition.

[1] A reduced version of the 57-bus benchmark due to Power World Licensing restrictions.

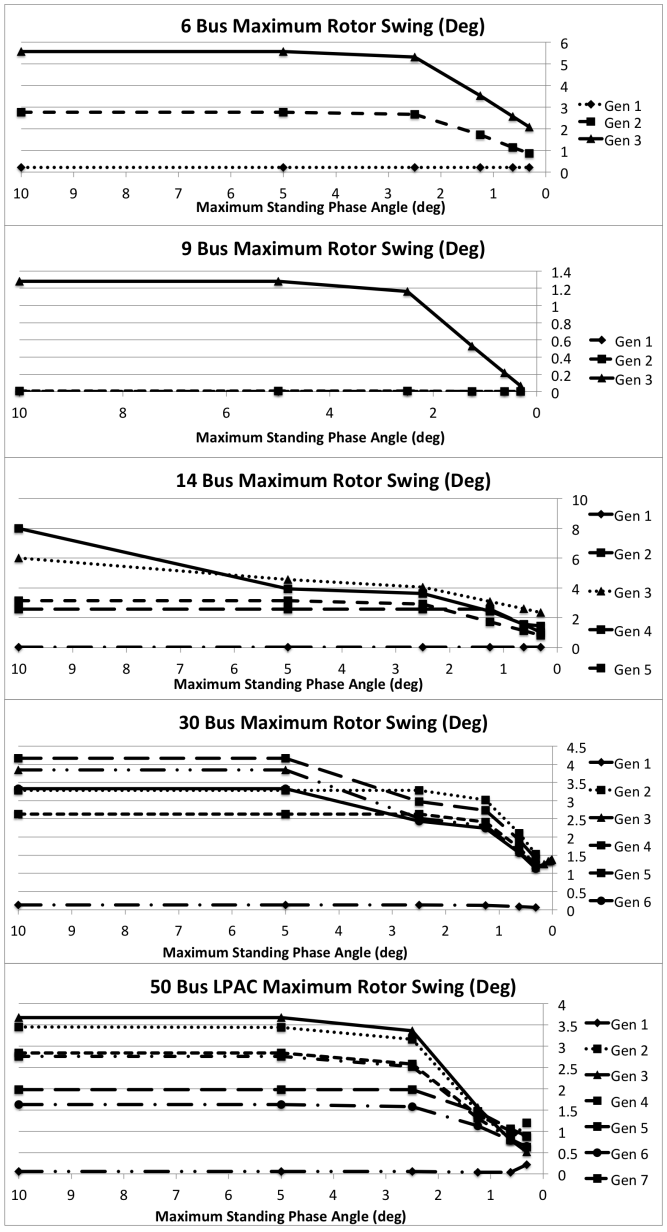

Fig. 6. Maximum Rotor Swing on a Fixed Restoration Order

Complete Search on the 6-Bus and 9-Bus Cases: Table VI and Figure 7 present the for the LPAC-ROP-SPA. Table VI, when compared to Table V, highlights the benefits of co-optimizing the restoration prioritization, as the blackout percentage is reduced by 3% and 12% in the 6-Bus and 9-Bus networks. Figure 7 shows also consistent monotonic reductions in rotor swings. Note that, although Figures 7 and 6 show similar trends, their values cannot be compared directly because the underlying restoration plans differ.

RAD on the 14-Bus, 30-Bus, and 50-Bus Cases: Consider now the larger benchmarks which are solved with randomized adaptive decomposition. Since this algorithm is randomized, it typically produces different results on each execution and provide no quality guarantees. This section reports only one run of the LPAC-ROP-SPA algorithm and hence these results must be seen as general trends on not precise values. Table

TABLE VI. RUNTIME & BLACKOUT ON OPTIMAL RESTORATION ORDERINGS FOR DECREASING SPA VALUES

	6 Bus			9 Bus		
θ^{Δ} Deg	Runtime (sec)	Blackout (%)	Δ (%)	Runtime (sec)	Blackout (%)	Δ (%)
180	1456.6237	29.1442	0.0000	558.8831	62.8310	0.0000
10	1233.9379	29.1442	0.0000	565.1245	62.8310	0.0000
5	1414.1866	29.1442	0.0000	493.2480	62.8310	0.0000
2.5	608.1933	30.2073	3.6478	557.0650	62.8310	0.0000
1.25	1206.0126	30.2668	3.8518	631.5468	62.8310	0.0000
0.625	1129.3481	30.3040	3.9795	615.6780	63.0012	0.2709
0.3125	1675.2234	30.4274	4.4028	753.1019	63.1087	0.4420

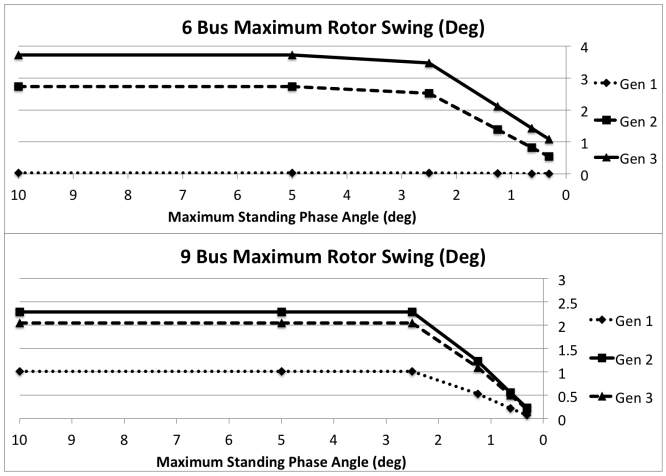

Fig. 7. Maximum Rotor Swing with Optimal Restoration Orderings

VII summarizes both the restoration plans and the rotor swings for the following step sizes: $\theta^{\Delta} = 180, 5, 0.625$. The results show the same trend as the smaller benchmarks: As the SPA constraints are tightened, the maximum rotor swings become smaller. However, the results also indicate that the SPA-constraints help in producing smaller blackout sizes. This counter-intuitive result is due to the limits on computation times and highlights that SPA-constraints can in fact drive the search towards high-quality restoration plans early, while the unconstrained algorithm may explore regions of the search space that may prove infeasible in later steps. Additional experiments are needed to confirm these observations generally but it is important to emphasize that LPAC-ROP-SPA has produced the best restoration plans on these case studies.

VII. THE IMPACT OF SVD CONSTRAINTS

This section considers SVD constraints motivated by the 39-Bus network which is unique for several reasons. First, it has 10 generators, significantly more than other benchmarks. Voltage bounds must be tightened from ± 0.06 V p.u. to ± 0.03 V p.u. to ensure convergence of LPAC-ROP-SPA plans to AC-feasible power flows. Finally, even with tight SPA constraints, the restoration plans produce significant rotor swings. After a detailed investigation, it appears that these swings are caused by significant differences between the voltages on the buses. This was the key motivation in introducing the LPAC-ROP-SPASVD formulation. Table VIII and Figure 8 present the restoration plan results for a fixed ordering on the 39-bus case with a standing voltage difference of $V^{\Delta} = 0.005$ V p.u. Figure 8 shows four representative generators from the 10 total generators in the network. The restoration plans are evaluated

TABLE VII. RUNTIME, BLACKOUT, & ROTOR SWINGS ON RAD FOR DECREASING SPA VALUES

θ^{Δ} Deg	Runtime(sec)	Blackout(%)	Gen 1	Gen 2	Gen 3	Gen 4	Gen 5	Gen 6	Gen 7
14 Bus (Limit: 2hr)									
180	5427.4266	7.0319	0.0326	2.5931	6.0216	7.9865	3.1483		
5	7200.0565	6.9732	0.0662	4.9771	3.6925	3.2947	4.5103		
0.625	7200.1826	6.7901	0.0167	1.1987	0.9181	0.8384	1.0966		
30 Bus (Limit 2hr)									
180	7204.1037	21.6491	0.1246	3.1934	3.8476	2.5767	4.1693	3.3256	
5	7205.7879	19.7539	0.2405	6.3994	3.9005	4.4040	4.2817	3.6690	
0.625	7214.5057	18.0415	0.2221	0.1504	1.5442	1.4733	0.6440	0.8368	
50 Bus (Limit 4hr)									
180	14478.9556	14.6031	0.0434	0.6521	3.8454	4.6441	5.7794	6.2289	7.6763
5	14403.3878	12.8734	0.0288	0.2012	0.6263	1.9467	2.9263	2.9146	3.3718
0.625	14439.8082	11.9223	0.0429	0.8242	2.4939	1.9590	1.8267	1.4765	1.6270

TABLE VIII. THE 39-BUS NEW ENGLAND TEST SYSTEM

	SPA Constraints			SPA and SVD Constraints		
θ^{Δ} Deg	Runtime (sec)	Blackout (%)	Δ (%)	Runtime (sec)	Blackout (%)	Δ (%)
180	7.4765	39.6525	0.0000	10.4956	39.7927	0.0000
10	7.6019	39.6525	0.0000	9.8277	39.7927	0.0000
5	8.2470	39.6535	0.0025	7.9990	39.7937	0.0025
2.5	7.6262	39.6778	0.0636	8.9144	39.8184	0.0645
1.25	7.7845	39.7399	0.2203	9.1230	39.8816	0.2234
0.625	7.6365	39.7782	0.3170	10.5470	39.9183	0.3157
0.3125	7.3960	39.7999	0.3716	10.1688	39.9385	0.3664

with just SPA constraints (replicating the experiment from Section VI-A) and again with the SPA and SVD constraint. With SPA constraints only, generators 6 and 7 behave just like the previous experiments but generators 2 and 4 are unique in that their rotor swings do not decrease with tighter SPA constraints. With SVD constraints, the SPA constraints control rotor swings more effectively. Interestingly, setting the SVD limit below 0.005 makes the LPAC-ROP-SPA infeasible. This is not surprising as voltages may not be effectively controlled by generator dispatch and load pickups: Local reactive power compensation is likely required for the feasibility of small SVD constraints. These results suggest that SPA constraints alone are not enough to ensure small rotor swings: It is advantageous to add SVD constraints to the ROP model and possibly to couple them with local reactive support.

VIII. CONCLUSION & FUTURE WORK

The Restoration Ordering Problem (ROP) prioritizes repairs for a transmission system after a significant disruption. It produces a sequence of AC-feasible steady states by jointly optimizing generator dispatch, load pickups, and restoration prioritization in order to minimize the size of the blackout while satisfying the network operational constraints. This paper focus on transient stability and determining whether it is possible to transition in between the steady states produced by the ROP. We propose a new generalization of the ROP, the AC-ROP-SPASVD problem, that splits restoration steps into dispatching and closing steps. The formulation uses standing phase angles constraints and voltage difference constraints as a surrogate for rotor swing reductions. We show that solutions from DC power flow approximation are not always feasible to convert to AC solutions and find that the SPA constraints on the DC power flow model cannot reduce rotor swings.

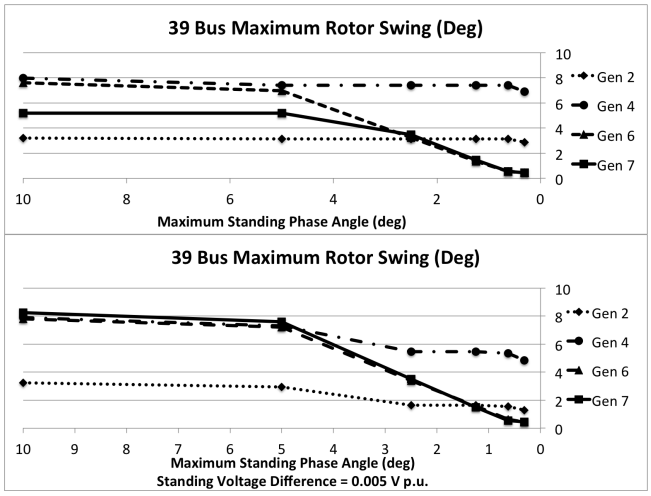

Fig. 8. Maximum Rotor Swing on 39 Bus: SPA Constraints (top), SPA and SVD Constraints (below)

By utilizing the LPAC model, case studies indicate that the novel AC-ROP-SPASVD formulation reduces rotor swings of synchronous generators by over 50%, while having a negligible impact on the blackout size (i.e., $\leq 1.5\%$ increase), which is still optimized holistically. We further illustrate in the 39-Bus benchmark that reducing standing phase angles is not a sufficient condition for reducing rotor swings. To address this limitations, we further introduce SVD constraints, which are effective in further reducing rotor swings. Our work is a first step in incorporating transient stability with power system restoration optimization. Exploring a tighter integration of transient simulations and optimizations for power system restoration will be our future goal. This would also enable us to handle future extensions, e.g. rotor shaft impacts (RSIs) [19].

ACKNOWLEDGEMENT

NICTA is funded by the Australian Government through the Department of Communications and the Australian Research Council through the ICT Centre of Excellence Program. NICTA is also funded and supported by the Australian Capital Territory, the New South Wales, Queensland and Victorian Governments, the Australian National University, the University of New South Wales, the University of Melbourne, the University of Queensland, the University of Sydney, Griffith University, Queensland University of Technology, Monash University and other university partners.

REFERENCES

[1] C. Coffrin, P. Van Hentenryck, and R. Bent, "Accurate Load and Generation Scheduling for Linearized DC Models with Contingencies," *Proceedings of the 2012 IEEE Power & Energy Society General Meetings (PES)*, 2012.

[2] ——, "Strategic stockpiling of power system supplies for disaster recovery." *Proceedings of the 2011 IEEE Power & Energy Society General Meetings (PES)*, 2011.

[3] P. Van Hentenryck, C. Coffrin, and R. Bent, "Vehicle routing for the last mile of power system restoration," in *PSCC'11, Stockholm, Sweden*.

[4] C. Coffrin and P. Van Hentenryck, "Feasible load and generation scheduling for transmission system restoration," in *PSCC'14, Wroclaw, Poland*, 2014.

[5] C. Coffrin and P. V. Hentenryck, "A linear-programming approximation of ac power flows," *Forthcoming in INFORMS Journal on Computing*, 2013.

[6] M. Adibi and R. Kafka, "Power system restoration issues," *Computer Applications in Power, IEEE*, vol. 4, no. 2, pp. 19–24, 1991.

[7] M. Adibi and L. Fink, "Power system restoration planning," *IEEE Transactions on Power Systems*, vol. 9, no. 1, pp. 22–28, 1994.

[8] D. Hazarika and A. Sinha, "An algorithm for standing phase angle reduction for power system restoration," *Power Systems, IEEE Transactions on*, vol. 14, no. 4, pp. 1213–1218, 1999.

[9] A. Ketabi, A. Ranjbar, and R. Feuillet, "New approach to standing phase angle reduction for power system restoration," *European transactions on electrical power*, vol. 12, no. 4, pp. 301–307, 2002.

[10] H. Ye and Y. Liu, "A new method for standing phase angle reduction in system restoration by incorporating load pickup as a control means," *International Journal of Electrical Power & Energy Systems*, vol. 53, pp. 664–674, 2013.

[11] "Powerworld simulator," PowerWorld Corporation, http://www.powerworld.com.

[12] R. P. Klump and J. D. Weber, "Real-time data retrieval and new visualization techniques for the energy industry," in *HICSS'02*, 2002.

[13] R. Zimmerman, C. Murillo-S andnchez, and R. Thomas, "Matpower: Steady-state operations, planning, and analysis tools for power systems research and education," *IEEE Transactions on Power Systems*, vol. 26, no. 1, pp. 12 –19, feb. 2011.

[14] P. Kundur, *Power system stability and control*. Tata McGraw-Hill Education, 1994.

[15] K.-H. Tseng, W.-S. Kao, and J.-R. Lin, "Load model effects on distance relay settings," *Power Delivery, IEEE Transactions on*, 18(4), 2003.

[16] R. Bent and P. Van Hentenryck, "Randomized adaptive spatial decoupling for large-scale vehicle routing with time windows." in *AAAI'07*, 2007, pp. 173–178.

[17] D. Pacino and P. Van Hentenryck, "Large neighborhood search and adaptive randomized decompositions for flexible job-shop scheduling," in *IJCAI'11*, 1997–2002, 2011.

[18] C. Coffrin, P. V. Hentenryck, and R. Bent, "Last-mile restoration for multiple interdependent infrastructures," in *AAAI*, 2012.

[19] N. Martins, E. J. de Oliveira, W. C. Moreira, J. L. R. Pereira, and R. M. Fontoura, "Redispatch to reduce rotor shaft impacts upon transmission loop closure," *Power Systems, IEEE Transactions on*, 23(2), pp. 592–600, 2003.